Focal Mechanism of Earthquakes on Island Arcs in the Southwest Pacific Region

By

Kazuo MINO, Toshiyuki ONOGUCHI and Takeshi MIKUMO

Disaster Prevention Research Institute, Kyoto University

(Manuscript Received September 3, 1968)

Abstract

The focal mechanisms of 33 earthquakes that occurred along island arcs from New Guinea to the Fiji Islands have been determined from the long-period seismograms of the World-Wide Standardized Seismograph Network and some other observations. The observed first motions of P waves show a quadrantal distribution for most of the earthquakes. The solutions for some earthquakes are also supported by the source amplitudes of P waves, which have been corrected for the effects of propagation and instrument. The polarization angles of S waves for several earthquakes suggest the double-couple type mechanism.

The axes of the maximum pressures inferred from a number of the solutions are oriented almost perpendicularly to the trend of the island arcs in some cases, but nearly parallel in other cases. The plunge of the pressure axis for most of intermediate and deep earthquakes appears to be parallel to the dip of the spatial distribution of foci.

1. Introduction

The mechanism of earthquakes in the circum-Pacific zone has come to receive recent attentions, particularly in relation to the tectonics of island arcs which are characterized by the existence of deep earthquakes, active volcanoes and oceanic trenches and are also noted for large gravity anomalies, abnormal heat flow, heterogeneous Q distribution and so forth.

The islands in the southwest Pacific region, extending from New Guinea-New Britain-Solomon-Santa Cruz-New Hebrides Islands to the Fiji-Tonga Islands, consist of a typical arcuate structure, and this zone is well-known as one of the most seimically active regions in the world for a great number of earthquakes with shallow to very deep origins (Sykes, 1966 ; Isacks *et al.*, 1967). This region provides, therefore, the best field for solving fundamental problems if there are any differences in the focal mechanism among shallow, intermediate and deep earthquakes, and their geophysical implications for the tectonic structure of island arcs. Although some seismologists have obtained fault plane solutions for earthquakes in some parts of this region (Schäffner, 1959, 1961 ; Scheidegger, 1959 ; Lensen, 1960 ; Ritsema, 1959, 1960 ; Hodgson *et al.*, 1962 ; Balakina, 1962), many of the solutions were based on a rather poor distribution of recording stations and somewhat less reliable observations made before the World-Wide Standardized Seismograph Network (WWSSN) was established.

In the present paper, the focal mechanism solutions for a number of earthquakes in the region are determined not only from the radiation pattern of

first motions of P waves but also from the polarization angles of S waves, mainly using the long-period seismograms obtained by the WWSSN. Further attempts are made to determine the source amplitudes from the records and to compare them with the corresponding theoretical amplitudes, in order to test the appropriateness of the solutions. Our main purpose here will be focused on the state of earthquake generating stresses and their relation to the general tectonics of the arcuate structure, through the distribution of the maximum pressure and tension axes derived from individual focal mechanisms.

Table 1. Information of the earthquakes mentioned in the present study.

Earthq. No.	Date	Origin time h m s	Location φ	λ
1	1963 Feb. 13	18 13 55.1	9.9° S	160.8° E
2	Feb. 26	20 14 08.7	7.5 S	146.2 E
3	Feb. 27	04 30 00.8	6.0 S	149.4 E
4	Mar. 30	01 53 28.8	19.1 S	169.1 E
5	May 1	10 03 20.0	19.0 S	169.0 E
6	July 4	10 58 13.2	26.3 S	177.7 W
7	Aug. 22	19 52 25.0	9.4 S	158.0 E
8	Sept. 15	00 46 54.1	10.3 S	165.6 E
9	Sept. 17	19 20 08.2	10.1 S	165.3 E
10	Nov. 4	01 14 32.8	15.1 S	167.3 E
11	1964 Jan. 14	15 38 13.9	5.2 S	150.8 E
12	Jan. 20	17 18 37.4	20.7 S	169.9 E
13	Feb. 14	16 29 45.0	5.1 S	151.7 E
14	Mar. 27	20 22 10.6	23.7 S	179.9 E
15	Apr. 24	05 56 10.1	5.1 S	144.2 E
16	July 9	16 39 49.3	15.5 S	167.6 E
17	Nov. 19	23 35 06.0	6.0 S	150.8 E
18	Dec. 7	08 58 45.8	5.4 S	151.3 E
19	1965 Mar. 24	07 59 39.0	16.3 S	167.9 E
20	Apr. 10	22 53 04.8	13.4 S	170.3 E
21	Aug. 29	13 57 20.2	17.7 S	178.9 E
22	1966 Jan. 28	11 39 02.1	10.2 S	161.2 E
23	Feb. 4	10 39 12.2	15.9 S	167.9 E
24	Feb. 22	05 02 27.2	5.4 S	151.5 E
25	May 21	08 08 30.6	24.3 S	179.8 E
26	June 4	08 35 11.4	14.8 S	171.2 E
27	July 10	01 22 02.9	17.4 S	178.7 W
28	Oct. 7	02 06 35.3	17.8 S	178.2 W
29	Nov. 6	14 43 16.6	17.9 S	178.8 W
30	Dec. 1	04 56 58.2	14.0 S	167.1 E
31	Dec. 30	01 00 25.4	17.8 S	178.9 W
32	1967 Feb. 14	05 02 38.4	13.3 S	171.3 E
33	June 21	19 10 31.1	23.5 S	180.0 E

2. Data

Data mainly used in the present study are the long-period seismograms which have been recorded at the WWSSN operated by the United States Coast and Geodetic Survey (USCGS). The seismograph-recording system at the stations has constants of $T_0 = 30$ sec, $T_g = 100$sec, $h_0 = h_g = 1$, and a magnification ranging from 750 to 3,000. In addition to the above data, we have also used the Earthquake Data Report (EDR) published by the USCGS and the Bulletin of the International Seismological Committee (BISC). For Japanese stations

Region	Focal Depth	Magnitude	Number of recording stations	Remarks
Solomon Is.	29	5.8	40	I, III
E. New Guinea	171	7.1	48	I , III
New Britain Is.	52	5.2	11	I
New Hebrides Is.	160	6.1	37	I , III
New Hebrides Is.	140	6.2	49	I , III
S Fiji Is.	158	6.5	67	I , III
Solomon Is.	33	6.1	17	I
Santa Cruz Is.	43	6.3	53	I , III
Santa Cruz Is.	17	6.1	70	I , III
New Hebrides Is.	154	5.8	11	I ,
New Britain Is.	109	5.6	23	I , III
New Hebrides Is.	141	6.1	66	I , III
New Britain Is.	55	6.0	67	I , III
Fiji Is.	520	5.0	30	III
New Guinea	106	6.5	65	I , III
New Hebrides Is.	121	(7.5)	68	I
New Britain Is.	33	6.0	61	I
New Britain Is.	54	5.8	28	I
New Hebrides Is.	189	5.6	11	II
New Hebrides Is.	644	6.2	11	II
Fiji Is.	571	5.4	13	II
Solomon Is.	33	5.6	14	II
New Hebrides Is.	190	6.0	28	I , II
New Britain Is.	28	6.2	15	II
Fiji Is.	518	5.1	10	II
New Hebrides Is.	660	4.6	11	II
Fiji Is.	532	5.8	15	II
Fiji Is.	639	4.8	13	II
Fiji Is.	548	4.7	12	II
New Hebrides Is.	132	(6.1)	51	I , II
Fiji Is.	658	5.0	14	II
New Hebrides Is.	635	5.6	20	II
Fiji Is.	546	5.0	15	II

more information was available from the Monthly Seismological Bulletin of the Japan Meteorological Agency. All of the above data cover the 5 year period from January 1963 to March 1967.

Out of a great number of earthquakes that occurred during the period along island arcs from New Guinea to the Fiji and Tonga Islands (0° - 27°S, 125° E - 170°W), almost all the earthquakes, whose magnitude was greater than 4.5 and for which a clear first motion of P waves (i_p) was observed at more than 10 stations, have been selected for the present purpose. Out of the total number of earthquakes selected amounting to about 160, the focal mechanism solution has been obtained for 33.

Table 1 gives the information pertinent to the earthquakes, including the origin times, locations of epicenter, focal depths and magnitudes determined by the USCGS. Remarks indicate the source of data ; I from the WWSSN records, II from the EDR, and III from the BISC. Fig. 1 shows the distribution of the epicenters of all the earthquakes studied. The spatial distribution

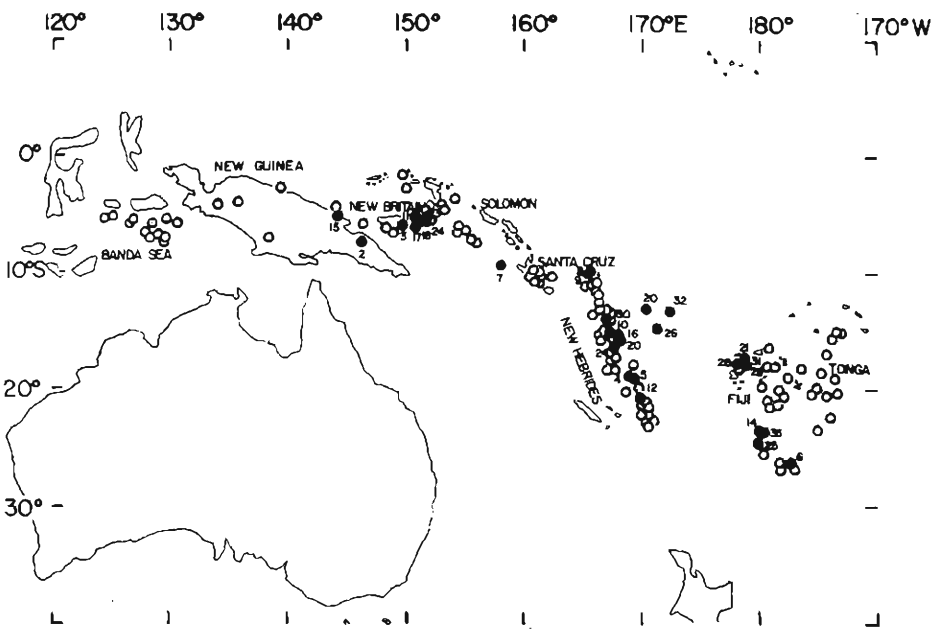

Fig. 1. Locations of the earthquakes mentioned in this paper. Solid circles indicate the earthquakes of which the focal mechanism has been determined.

of the foci on the vertical profiles along the east-west and north-south directions is illustrated in Figs. 2 (a) and (b) respectively. It may be seen from these figures that many of the earthquakes took place along the island arcs and trenches in the shallow crust and down to about 600 km in the upper mantle. Solid circles indicate the earthquakes of which the focal mechanism has been determined. It may be reasonable to suppose from the distribution that the mechanisms of the earthquakes could be representative of those for many earthquakes in this region.

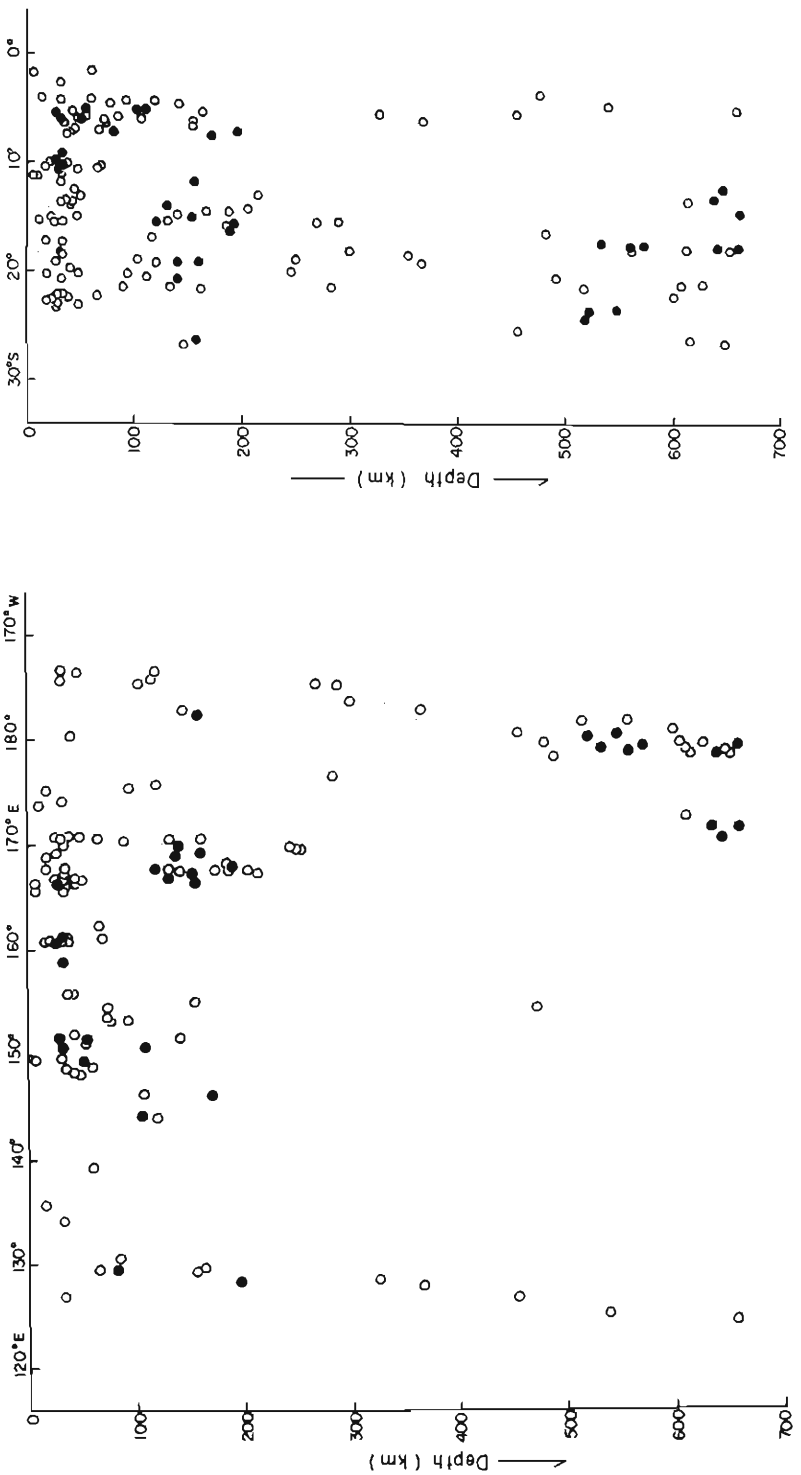

Fig. 2 Vertical cross-sections of the spatial distribution of foci
(a) East-west profile.
(b) North-south profile.

3. Method of Analysis

The focal mechanism is investigated by the following methods using information from P and S waves.

1. P wave first motion

The polarity of the first motion of P or PKP waves is mainly determined on the vertical component seismograms with some reference to two horizontal records. In order to get a clear picture of the radiation pattern of the first motions, we use the Wulff-net projection here, on which all recording stations are plotted inside a unit circle, according to the emergent angle determined from the velocity structure. Ritsema's $i-\Delta$ curve (1958) is used for this purpose. Theoretically, the P wave first motions should give the same quadrantal pattern for the single couple and double couple type mechanisms, so that the type of source models cannot be determined solely from P wave observations.

2. S wave polarization

Although S waves play an important rôle in the determination of focal mechanism, it is usually difficult to determine the polarity or amplitude of the initial S phase with high reliability. In the present study, the polarization angle, indicating the major direction of oscillation of the S wave group, is used as additional information for several earthquakes. The angle, which is related to the ratio of the amplitude of SH to that of the SV component, may be determined from the relation, $\tan \varepsilon = SH/SV = \cos i_0 \cdot \tan \gamma_0$ (Stauder, 1960), knowing the angle γ_0 between the azimuth to the epicenter and the main direction of S particle motion, and the angle of incidence i_0 of a ray to the earth's surface. γ_0 can be measured from a vectorial combination of two horizontal records of S waves. For the single couple source, traces of the direction of S wave polarization converge to the pole of motion, while for the double couplemodel they converge to the intersections of the tension axis with the focal sphere and diverge from the axis of compression stress (stauder, 1960).

3. P wave source amplitude

For some earthquakes, the initial portion of P waves recorded at a number of stations are analysed by the Fourier transform to obtain the source amplitude spectrum, which provides a test for focal mechanism solutions. The wave emitted from the source will be subjected to various effects during the passage to a recording station, in the following way (Teng and Ben-Menahem, 1965),

$$S(\omega) \rightarrow P(\omega) \rightarrow C(\omega) \rightarrow I(\omega) \rightarrow A(\omega)$$

where $S(\omega)$; source spectrum
$P(\omega)$; effects of propagation including geometrical spreading and attenuation
$C(\omega)$; effects of crustal layering under the recording station
$I(\omega)$; instrumental response
$A(\omega)$; observed spectrum

The source spectrum should therefore be obtained by

$$S(\omega) = A(\omega) / (P(\omega) \cdot C(\omega) \cdot I(\omega)),$$

from the observed spectrum by removing the above effects. The source amplitudes for some specific frequencies thus obtained are compared with the theoretical amplitudes based on a focal mechanism solution appropriate to the earthquake studied, on the assumption that the waves are radiated to all direc-

tions with the same source function. Since the crustal structures under recording stations are not known very accurately, corrections of the observed amplitudes have been made for different crustal models. Solid circles in Figs. 5 and 17 indicate the amplitudes corrected for a unilayered crust * which is applied to all stations, while open circles correspond to those for multilayered crustal models appropriate to each recording site based on various sources of information. For the attenuation effects included in $P(\omega)$, we use a Q model (Model 5) (Mikumo and Kurita, 1968) for the whole mantle. More detailed discussion of the source spectrum will be given in a separate paper (Mikumo *et al.*).

4. Focal Mechanism

In this section, the focal mechanism of each earthquake or group of earthquakes is determined mainly from the distribution of the P wave first motion, together with S wave polarizations and P wave source amplitudes. The orientations of maximum pressure and tension axes are also estimated from the solutions to discuss the earthquake generating stresses. In some cases, a single solution has been derived from a group of earthquakes by superposing the first motion distributions. The superposition was made for earthquakes having an apparently similar first motion pattern and with actually the same location and similar focal depths. If inconsistent signs of the first motion

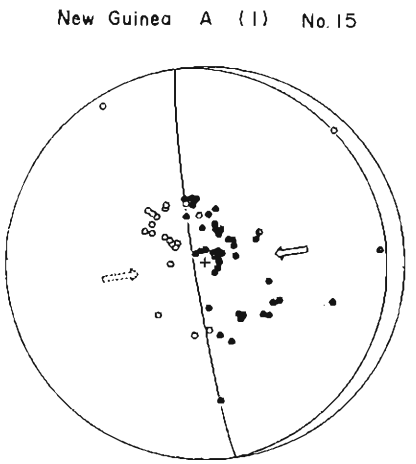

Fig. 3. Radiation pattern of P wave first motions projected on the lower half of the Wulff-net. solid circles : rarefactions, open circles : compressions. The arrows show the direction of the maximum pressure. The same explanations apply to Figs. 6, 7, 8, 9, 10, 13, 14, 15, 18, 19, 20, 21, 22.

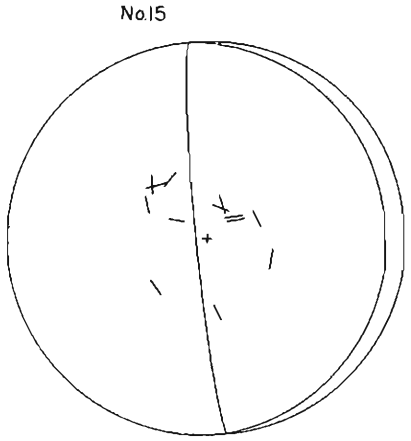

Fig. 4. S wave polarization angles.

* $Vp_1 = 6.28$ km/sec, $Vs_1 = 3.63$ km/sec, $\rho_1 = 2.87$ g/cm^3, $H = 37.0$ km
$Vp_2 = 7.96$ km/sec, $Vs_2 = 4.60$ km/sec, $\rho_2 = 3.37$ g/cm^3,

exceeded 10%, the superposed results have been discarded. In the figures that follow, open and solid circles show compression and rarefaction respectively, on the lower focal hemisphere of the Wulff net.

1. New Guinea

Four earthquakes were studied for this region, and the focal mechanism solution was obtained for earthquakes No. 2 and No. 15.

For earthquake No. 15 two nodal planes, one dipping steeply and the other nearly horizontal, can be determined with small uncertainty from the first motion distributions as shown in Fig. 3. It appears that the polarization angles of the *S* waves, as given in Fig. 4, are consistent with the double couple type mechanism. Fig. 5 shows a comparison between the source amplitudes for a period of 20 sec derived from the observed records and the theoretical amplitudes based on the above solution. These amplitudes have been normalized at a reference station (MAN ; $\Delta = 30°.2$, $Az = 311°$). A rather linear relation seems to give support to the solution obtained, although some of the points plotted are sensitive to the choice of crustal models. For other periods we have a similar relation, but the points scatter over a wider range.

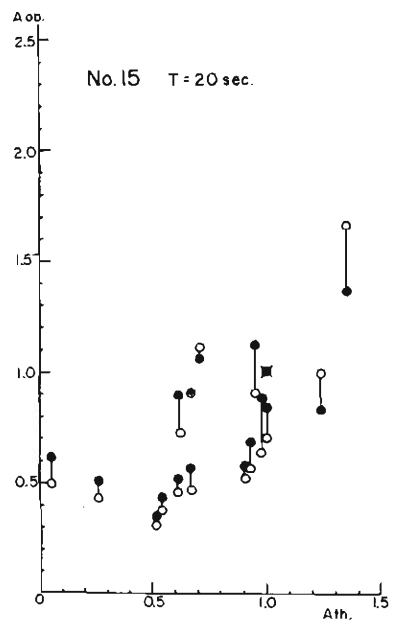

Fig. 5. Relation between the source amplitudes from observations and the theoretical amplitudes based on the solution for earthquake No. 15. Solid and open circles correspond to the unilayered and multilayered crustal models, respectively.

For earthquake No. 2, the strike of a steeply dipping plane, and hence the maximum pressure axis, runs almost parallel to that for earthquake No. 15. For the other two earthquakes not discussed here, any definite solution could not be determined because of great uncertainty.

2. New Britain

Eight earthquakes were investigated. Two solutions were obtained by superposing the first motion distributions for three earthquakes respectively.

For earthquake group A (Nos. 13, 18 and 24), a quadrantal pattern can be seen from Fig. 6. There is a small uncertainty for a nodal plane striking in the east-west direction, but another plane is hard to determine with a high precision. Fig. 7 shows the mechanism solution for another group B (Nos. 3, 11 and 17), which has a nearly vertical tension axis as in the case of A. The axis of maximum pressure for group B seems to be almost normal to that of A, but this situation could be changed to some extent, according to the accuracy in the determination of another plane in group A. The solution of the other two earthquakes could not be determined due to the poor distribution of recording stations.

3. Solomons

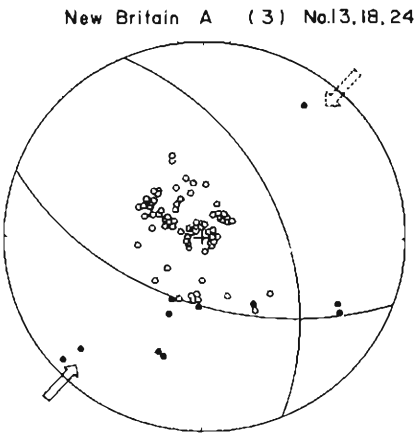

Fig. 6.

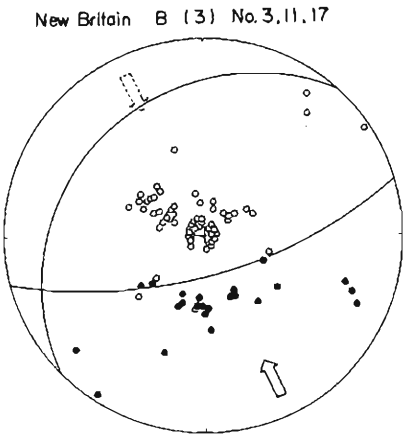

Fig. 7.

In the Solomon Island region seven earthquakes were included. Two solutions were obtained for earthquake group A (No. 1) and group B (No. 7 and No. 11). For earthquake No. 1 with a shallow origin under the island arc, two nodal planes can be determined with medium uncertainty. The maximum pressure axis is oriented nearly horizontally, whereas the maximum tension works along the vertical, as may be seen in Fig. 8. Earthquake group B has a similar radiation pattern. These two earthquake groups seem to be subjected to the same mechanism. Concerning the other four earthquakes, we do not have enough observations to arrive at a definite solution.

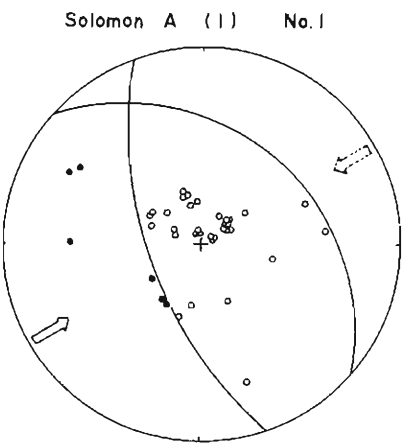

Fig. 8.

4. Santa Cruz

Four earthquakes were investigated. Figs. 9 and 10 show the distribution of the first motions for earthquakes No. 8 and No. 9 respectively. In these two earthquakes with almost the same location and shallow foci, an interesting feature is that the first motions of *P* waves were observed as rarefactions at all stations except in one or two BISC compression reports. If the double couple type mechanism is assumed, there is great arbitrariness in determinig two nodal planes, although the dip angle of each plane seems to be restricted to around 45 degrees, suggesting a near-vertical axis of the greatest pressure. The *S* wave polarization in both earthquakes shows, however, a concentration towards the epicenter or a strongly *SV*-polarized motion, as may be seen in Figs. 11 and 12 respectively, and it does not make any contribution to the precise determination of the nodal planes. There is a possibility that the mechanism of these two earthquakes could be explained by alternative hypotheses, such as a single force working vertically upwards at the focus or

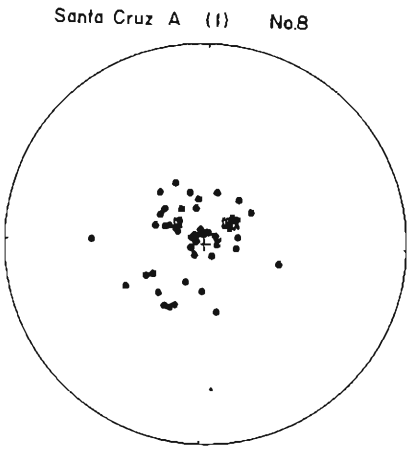

Fig. 9.

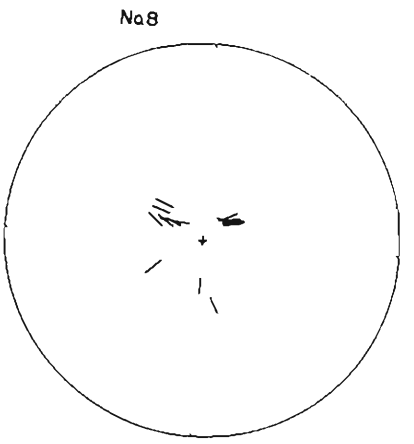

Fig. 11. *S* wave polarization angles.

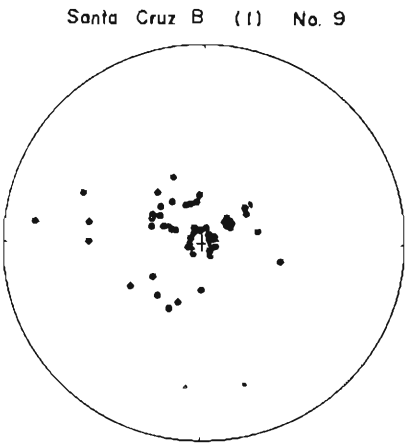

Fig. 10.

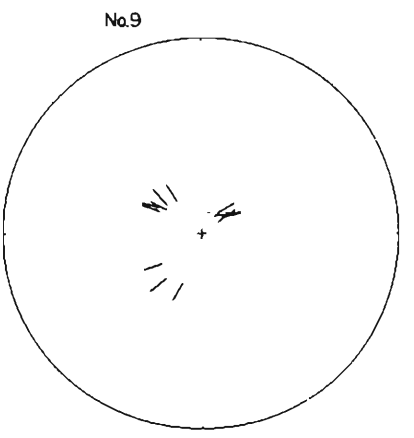

Fig. 12. *S* wave polarization angles.

the cone type mechanism. For the other two earthquakes, there is no systematic pattern in the first motion distributions.

5. New Hebrides

In this region six focal mechanism solutions were obtained from 15 earthquakes. Earthquake group A, a superposition of three earthquakes (Nos. 10, 16 and 30) with intermediate depths, has a solution with a nearly vertical tension axis and horizontal pressure axis striking in the NW-SE direction, as shown in Fig. 13. For earthquake group B including three deep-focus earthquakes (Nos. 20, 26 and 32), a quadrantal type solution may be obtained as illustrated in Fig. 14, although rarefaction data are not sufficient to assure a unique solution.

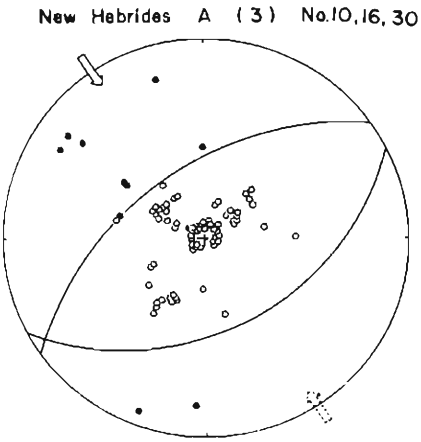

Fig. 13.

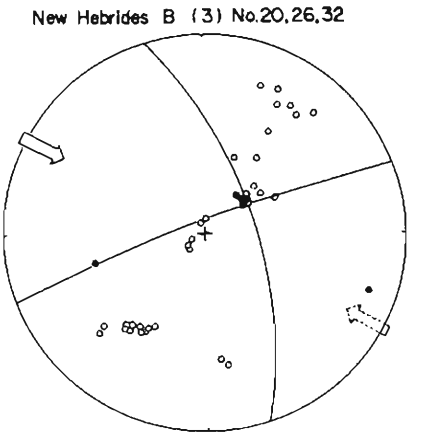

Fig. 14.

The WWSSN provides plenty of clear first motions for earthquake No. 12. Two nodal planes can be determined with minimum uncertainty, indicating a quadrantal type as seen in Fig. 15. Fig. 16 shows the pattern of S wave

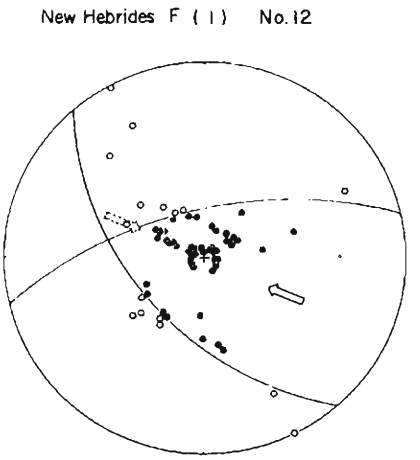

Fig. 15.

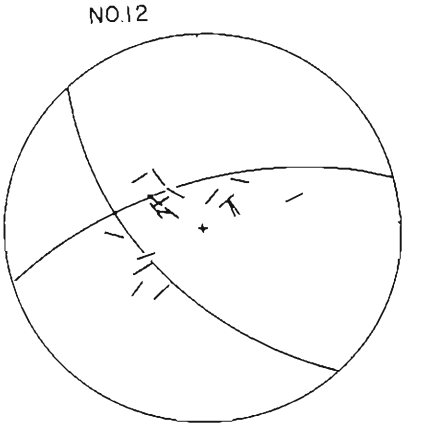

Fig. 16. S wave polarization angles.

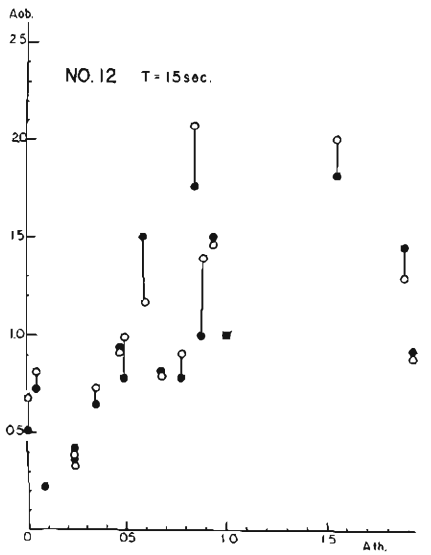

Fig. 17. Relation between the source amplitudes from observations and the theoretical amplitudes based on the solution for earthquake No. 12.

polarization, which appears to be consistent again with the double couple source. The source amplitudes from observations for a period of 15 sec and the theoretical amplitudes derived from the solution are compared with each other in Fig. 17, after normalization has been made for both kinds of amplitudes at a reference station (CMO, $\Delta = 91°.3$, $Az = 16°.7$). If a few points are excluded, there seems to be a linear relation which supports the above solution. Earthquake No. 5 also show a quadrantal pattern for P waves, as can be seen in Fig. 18. It is noticed, however, that the above two earthquakes with nearly the same location and intermediate depths show an almost opposite pattern for the observed first motions of P waves. This implies that the maximum pressure axes of the two shocks are nearly perpendicular to each other, and that the tension axis for earthquake No. 12 is almost parallel to the pressure axis for earthquake No. 5.

For earthquake group C (No. 19 and No. 23), two steeply dipping nodal planes are determined, as given in Fig. 19. Both the pressure and tension axes are nearly horizontal. A quadrantal solution is obtained with rather large uncertainty for group D (No. 4). For the other four earthquakes no satisfactory solutions were obtained.

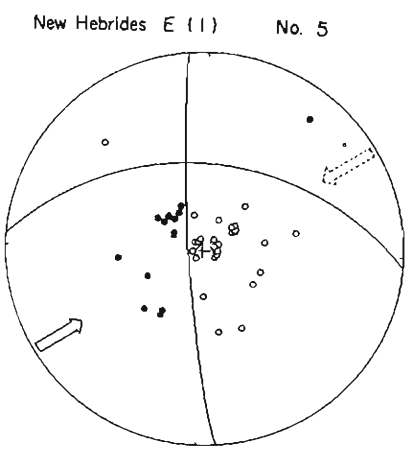

Fig. 18.

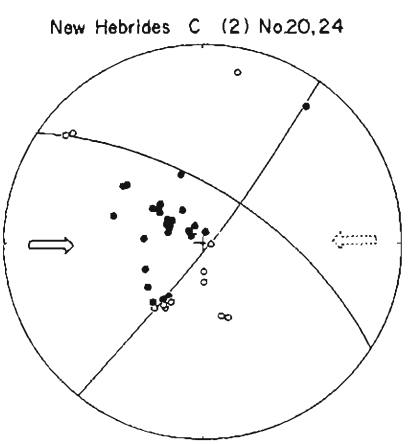

Fig. 19.

6. Fiji

Three solutions were obtained by superposing several earthquakes respectively out of the 19 earthquakes studied.

Earthquake group A (Nos. 14, 25 and 33) and group B (Nos. 21, 27, 28, 29, and 31), both with focal depths greater than 500 km, show a rather similar first motion pattern, which may be seen from Fig. 20 and 21. However,

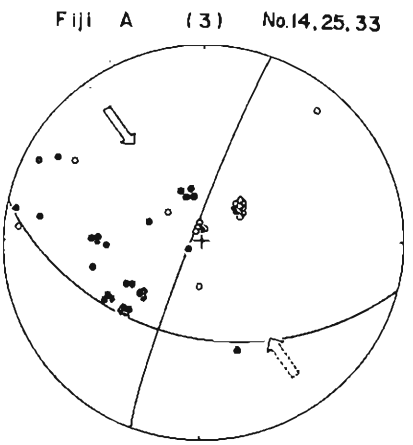

Fig. 20.

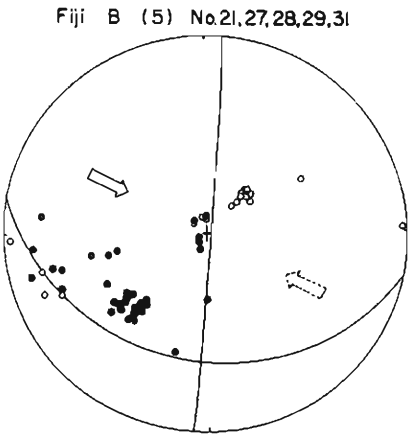

Fig. 21.

these two solutions are not definite ones in view of the poor distribution of stations. For earthquake No. 6, there is small uncertainty for one nodal plane striking in the east-west direction, but it is hard to fix another plane even if the source amplitudes are also taken into account. For the other 10 earthquakes in this region, no solutions could be obtained, probably because of the poor quality of the observation reports.

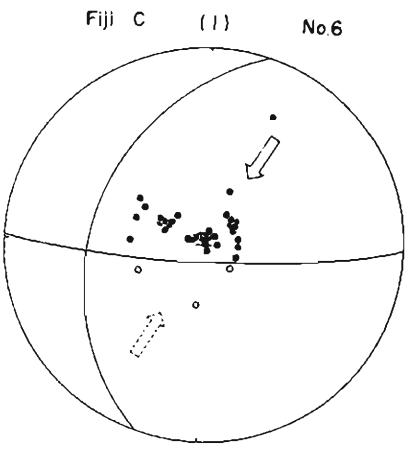

Fig. 22.

In addition to the above mentioned earthquakes, the focal mechanisms of six earthquakes with shallow and intermediate depths in the Tongan region have been examined. No satisfactory solutions were obtained, however, owing to the rather irregular patterns of first motion data.

5. Tectonic Stresses

The focal mechanism solutions obtained above give the general trend of orientation of the maximum pressure and tension axes for the earthquakes,

which may be indications of regional tectonic stresses working in this area. The results obtained are tabulated in Table 2 together with their uncertainty. This uncertainty means maximum variations determined visually and does not include any statistical meanings.

Table 2. Focal mechanism solutions.

Region	Earthq. No.		Max. pressure axis strike	Max. pressure axis plunge	Plane A strike	Plane A dip	Plane B strike	Plane B dip	Number of solutions	Number of the earthquakes studied
New Guinea	A	15	80°± 0°	52°±0°	171°± 0°	83°±0°	171°± 0°	6°± 0°	2	4
	B	2	65°±16°	38°±6°	173°± 0°	90°±0°	83°± 0°	22°±22°		
New Britain	A	13, 18, 24	232°±10°	6°±4°	155°±13°	46°±6°	109°± 0°	54°± 0°	2	8
	B	3, 11, 17	154°±3°	22°±1°	39°±10°	25°±3°	73°± 0°	70°± 0°		
Solomons	A	1	240°±15°	14°±6°	163°± 3°	63°±1°	120°±14°	36°± 6°	2	7
	B	7, 22	226°± 8°	10°±1°	134°±16°	37°±1°	139°± 0°	54°± 0°		
Santa Cruz	A	8							2	4
	B	9								
New Hebrides	A	10, 16, 30	321°±15°	6°±1°	50°±17°	42°±0°	55°± 0°	52°± 0°	6	15
	B	20, 26, 32	300°± 0°	14°±0°	162°± 0°	62°±0°	69°± 0°	82°± 0°		
	C	19, 23	264°± 0°	28°±0°	37°± 0°	86°±0°	124°± 0°	62°± 0°		
	D	4	250°± 4°	35°±0°	118°± 7°	25°±1°	176°± 0°	86°± 0°		
	E	5	237°±12°	20°±9°	181°± 7°	80°±3°	104°±11°	30°± 1°		
	F	12	115°± 0°	50°±0°	76°± 0°	63°±0°	139°± 0°	50°± 0°		
Fiji	A	14, 25, 33	322°± 3°	26°±3°	103°± 0°	37°±0°	27°± 3°	80°± 2°	3	19
	B	21, 27, 28, 29, 31	278°± 7°	48°±3°	5°± 0°	86°±0°	101°±16°	23°±14°		
	C	6	20°±15°	55°±9°	90°± 0°	80°±0°	67°±57°	12°±17°		

The strike of nodal planes and of maximum pressure is measured clockwise from the north, and the dip is measured by the angle between the nodal plane and the horizontal plane.

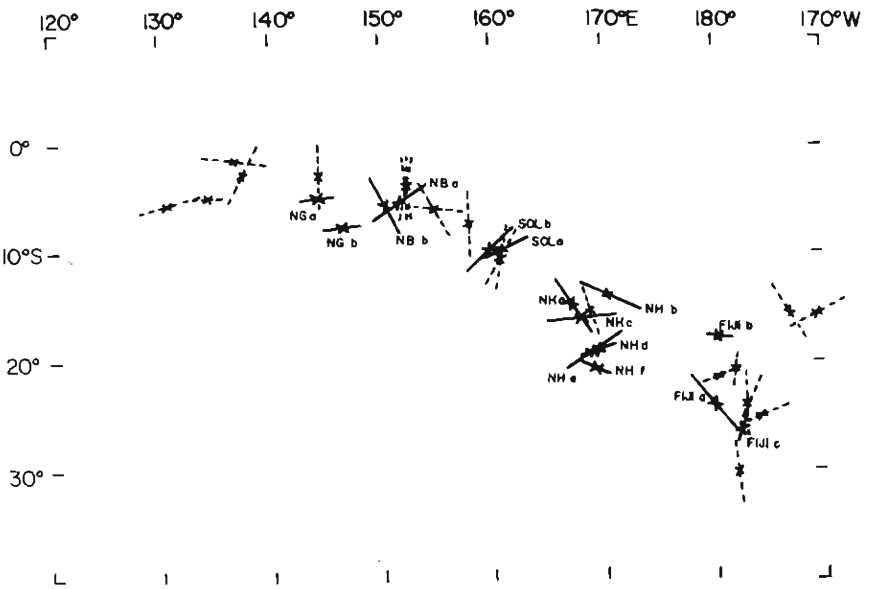

Fig. 23. Direction of the horizontal component of the maximum pressures.

The horizontal components of the maximum pressures are plotted in Fig. 23, by solid arrows placed at the center of the earthquakes investigated. Figs. 24 (a) and (b) indicate the corresponding pressure axes projected onto the vertical cross sections in the east-west (a) and north-south (b) directions respectively. Long arrows, short arrows and open circles correspond to cases where the angle between the axis and the projected plane is less than 30 degrees, between 30 and 60 degrees, and greater than 60 degrees, respectively. Dashed arrows are taken from Fara's catalogue (1964) of the fault plane solutions given by various authors for the 7.5 year period from January 1955 to August 1962.

A close examination of the horizontal distribution shows that some of the pressure axes are nearly perpendicular to the island arcs but that others are almost parallel to the trend of the arcs. For shallow earthquakes the axes are directed nearly horizontally. In earthquakes No. 8 and No. 9 in the Santa Cruz region, however, the pressure axis would be oriented vertically, if the double couple mechanism is assumed. It is interesting to note that the plunge of the pressure axis for most of intermediate and deep earthquakes seems to accord with the dip of the spatial distribution of the foci or the seismic zone, if the results summarized by Fara are incorporated into our analysis. It is to be also mentioned here that the maximum pressure axis for earthquake No. 5 in the New Hebrides Islands lies along the general direction, while that for earthquake No. 12, which has been supported by the amplitudes of P waves and the polarization of S waves, intersects normally to this direction, although the two earthquakes are not more than 1 degree apart from each other. This fact suggests that there might be two systems in the tectonic stress around this region. The distribution of the maximum tension axes has also been examined, but the results do not indicate any systematic patterns.

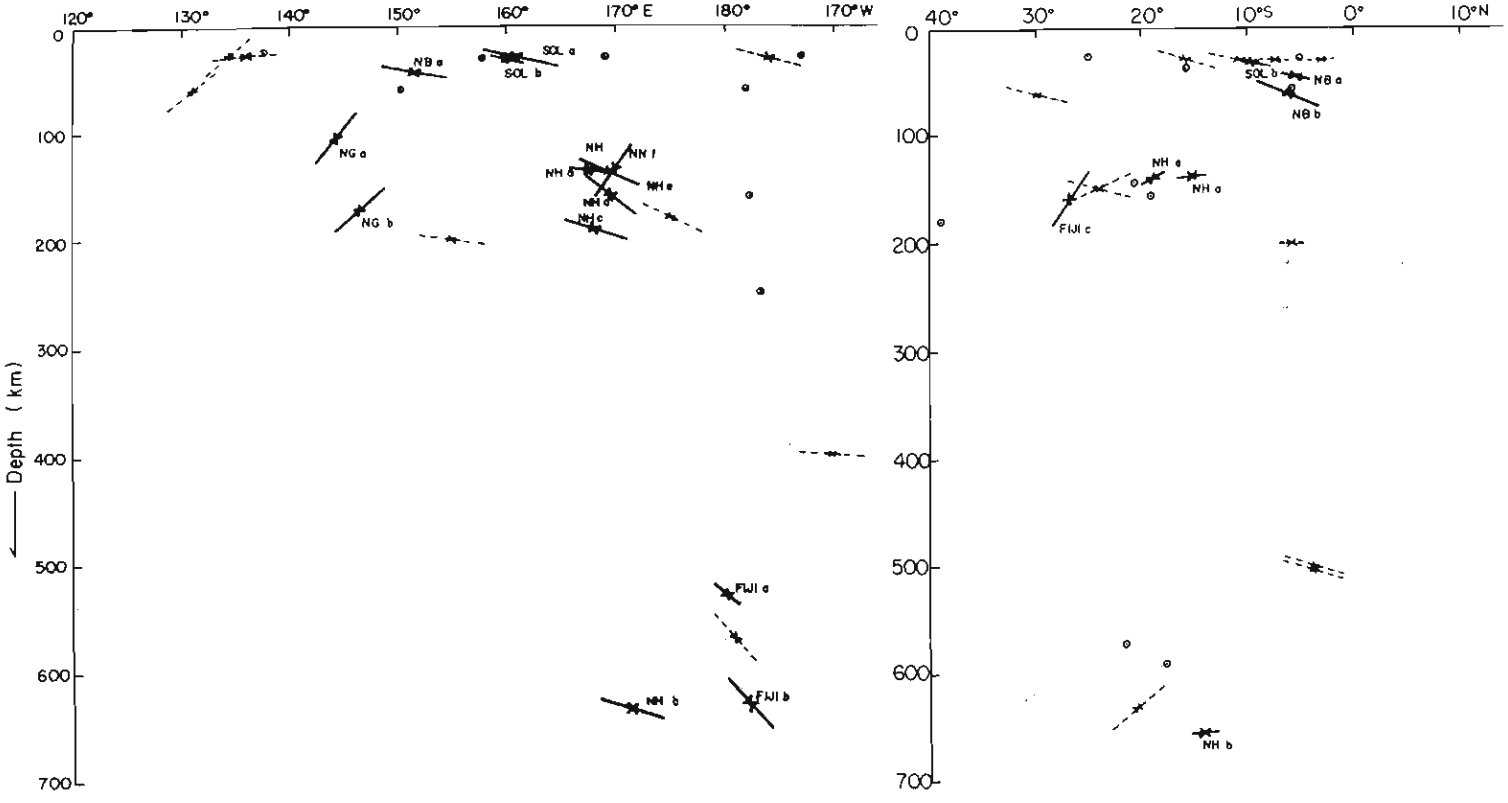

Fig. 24. Direction of the maximum pressures projected onto the vertical cross sections
(a) East-west profile, (b) North-south profile.

6. Discussion and Concluding Remarks

In the present study, 19 reliable solutions of the focal mechanism have been obtained for 33 earthquakes, mainly from the first motion pattern of individual earthquakes or in some cases of a group of earthquakes.

In the latter cases a superposition of first motion distribution has been made, on the assumption that these earthquakes may have the same mechanism. This attempt, however, has failed in some cases. Although it might be reasonable to make such an assumption for aftershocks, multiple shocks or earthquakes with spatial and temporal clusterings (Isacks *et al.*, 1967), there could be entirely different mechanisms due to variations in tectonic stresses even for earthquakes having actually the same location, if they occurred at different times. Such an example as has been demonstrated in the case of earthquakes No. 5 and No. 12 suggests a limit to the validity of the superposition.

The polarization of S waves has been examined for several earthquakes. The general pattern of polarization seems consistent with the solutions from P waves, suggesting the double couple type mechanism. It may be worthwhile, however, to note the strongly SV-polarized S waves in earthquakes No. 8 and No. 9. The same patterns have been observed before for several Kamchatka earthquakes (Stauder, 1960, 1962), but the present features are different from those cases in that the polarizations are directed towards the center of a rarefaction zone of P waves. The possibility of unusual focal mechanisms cannot be ruled out.

The source amplitudes of P waves for several periods have been used as a test of the mechanism solutions obtained. More complete analyses will be needed not only for the amplitude spectrum but for the phase spectrum over a wide range of frequencies or for the source function in the time domain, to compare with theoretical amplitudes with possible azimuthal dependence of frequency from volume sources.

The double couple mechanism can be associated with the fault motion or the equivalent shear dislocation along a slip plane. However, the focal mechanism studies using P and S waves do not give a unique solution to the problem of which of two nodal planes may correspond to the fault plane, without any assumptions about the relation between the solution and some geological features. Much previous work of this kind might have been biased by taking a favored choice from two possibilities. In the present study, no attempt has been made to determine the strike and dip of fault planes or the type of fault motion such as strike-slip or dip-slip. As might be seen from the solutions given in Table 2, however, there seems to be no predominant tendency in the strikes of the nodal planes, even if we take one preferred orientation of the two. Some seismologists have also emphasized the significance of the null vector for determining the type of fault motions and its relation with the trend of geological structure in the New Zealand - Kermadec - Tonga - Fiji - New Hebrides region (Hodgson, 1959 ; McIntyre and Christie, 1959), but no definite pattern could be detected for the whole region dealt with in this study.

The results obtained from the mechanism solutions are not sufficient to draw

definite conclusions about their relation with the tectonics of the island arc, but several features have been noticed in the present analysis, together with those in similar studies given by various authors (Fara, 1964). The focal mechanism studies thus far made in other regions (Honda and Masatsuka, 1952 ; Honda *et al.*, 1956 ; Balakina *et al* 1960 ; Ichikawa, 1961, 1966) have shown that mean directions of horizontal component of the maximum pressure are nearly perpendicular to the trend of deep and intermediate earthquake zones. In the present case, however, some of the pressure axes are oriented parallel to the trend, indicating the possible existence of a different system of tectonic stresses. A remarkable feature of the present result is that the general directions of the plunge of pressure axes appear to be parallel to the spatial distribution of foci or the 'seismic plane', as has been pointed out for deep and intermediate earthquakes near Japan (Ichikawa, 1961, 1966).

There is no systematic pattern, on the other hand, in the distribution of the tension axes in relation to the tectonic structure or focal distribution. This also agrees with the results given by some of the above authors. These situations imply that principal pressure, not principal tension, acts as an apparent earthquake generating stress in this region. Recently, Isacks and others (1968) analysed the mechanism of 6 intermediate and 15 deep-focus earthquakes in the Fiji-Tonga-Kermadec region, and also found that the axes of compression tend to be roughly parallel to the dip of the seismic zone.

A hypothesis that could account for the parallel alignment of the pressure axes on the 'seismic plane' has been presented recently (Sugimura and Uyeda, 1967), which associates a fault plane with the preferred orientation of olivine under regional stresses from the upper mantle convection current. An alternative interpretation (Isacks *et al.*, 1968) is that the deep seismic zone under island arcs is a downward moving segment of lithosphere, and that the mechanism of deep earthquakes indicates a compressional stress in the segment, being parallel to the presumed downward motion.

More focal mechanism solutions in each of the divided regions are required in order to obtain a conclusion about the above problems.

Acknowledgments

We wish to thank Dr. L. R. Sykes and Dr. M. Ichikawa for several comments on the manuscript. Our thanks are also due Mrs. R. Koizumi for arrangements of the material used. In the present study, we are much indebted for the seismograms supplied by the United States Coast and Geodetic Survey.

References

Balakina, L. M., H. I. Shirokova and A. V. Vvedenskaya, 1960, Study of stresses and ruptures in earthquake foci with the help of dislocation theory, Publ. Dominion Obs., **24**, 321-327.

Balakina, L. M., 1962, General regularities in the direction of the principal stresses effective in the earthquake foci of the seismic belt of the Pacific ocean, Izv. Akad. Nauk, SSSR, Ser. Geofiz., 1471-1483. (English translation)

Fara, H. D., 1964, A new catalogue of earthquake fault plane solutions, Bull. Seism. Soc. Am., **54**, 1491-1517.

Hodgson, J. H., 1959, The null vector as a guide to regional tectonic patterns, Publ. Dominion Obs., **20**, 369-384.

Hodgson, J. H., A. E. Stevens and M. E. Metzger, 1962, Direction of faulting in some of the large earthquakes of 1956-7, Publ. Dominion Obs., **26**, 229-269.

Honda, H. and A. Masatsuka, 1952, On the mechanism of the earthquakes and the stresses producing them in Japan and its vicinity, Sci. Rep. Tôhoku Univ., Ser. 5, **4**, 42-60.

Honda, H., A. Masatsuka and K. Emura, 1956, On the mechanism of the earthquakes and stresses producing them in Japan and its vicinity (second paper), Sci. Rep. Tôhoku Univ., Ser. 5, **8**, 186-205.

Ichikawa, M., 1961, On the mechanism of the earthquakes in and near Japan during the period from 1950 to 1957, Geophys. Mag., **30**, 355-403.

Ichikawa, M., 1966, Mechanism of earthquakes occurring in and near Japan, 1950-1962, Pap. Met. Geophys., **16**, 201-229.

Isacks, B. L., L. R. Sykes and J. Oliver, 1967, Spatial and temporal clustering of deep and shallow earthquakes in the Fiji-Tonga-Kermadec region, Bull. Seism. Soc. Am., **57**, 935-958.

Isacks, B. L., L. R. Sykes and J. Oliver, 1968, Focal mechanism of deep and shallow earthquakes in the Tonga-Kermadec region and the tectonics of island arcs, (in press).

Lensen, G. J., 1960, Principal horizontal stress directions as an aid to the study of crustal deformation, Publ. Dominion Obs., **24**, 389-397.

McIntyre, D. B. and J. M. Christie, 1959, The kinematics of faulting from seismic data, Publ. Dominion Obs., **20**, 385-393.

Mikumo, T., and T. Kurita, 1968, Q distribution for long-period P waves in the mantle, J. Phys. Earth, **16**, 11-29.

Ritsema, A. R., 1958, (i, Δ) curves for bodily seismic waves of any focal depth, Verhand. Meteorol. Geofisik. Inst., Djakarta, 54.

Ritsema, A. R., 1959, On the focal mechanism of southeast Asian earthquakes, Publ. Dominion Obs., **20**, 341-368.

Ritsema, A. R., 1960, Further focal mechanism studies at DeBilt, Publ. Dominion Obs., **24**, 355-358.

Schäffner, H. J., 1959, Die Grundlagen und Auswerterverfahren zur Seismischen Bestimmung von Erdbebenmechanismen, Freiberger Forschungshefte, C **63**, 1-183.

Schäffner, H. J., 1961, Tabellen kinematischer Erdbebenherdparameter, Publ. Inst. Angew. Geophys. Freiberg.

Scheidegger, A. E., 1959, Statistical analysis of recent fault plane solutions of earthquakes, Bull. Seism. Soc. Am., **49**, 337-347.

Stauder, W., 1960, An application of S waves to focal mechanism studies, Publ. Dominion Obs., **24**, 343-354.

Stauder, W., 1962, S-wave studies of earthquakes of the north Pacific, Part I: Kamchatka, Bull. Seism. Soc. Am., **52**, 527-550.

Sugimura, A. and S. Uyeda, 1967, A possible anisotropy of the upper mantle accounting for deep earthquake faulting, Tectonophysics, **5**, 25-33.

Sykes, L. R., 1966, The seismicity and deep structure of island arcs, J. Geophys. Res., **71**, 2981-3006.

Teng, T. L. and A. Ben-Menahem, 1965, Mechanism of deep earthquakes from spectrums of isolated body-wave signals, 1. Banda sea earthquake of March 21, 1964, J. Geophys. Res., **70**, 5157-5170.